Supporting Information

Engineering atomically dispersed Fe sites into TiO_2 for largely enhanced photocatalytic CO_2 reduction to CH_4

Wenlong Yang,[a] Zhenghui Ma,[a] Guoli Fan [a,b]*, Xiaoyan Pu,[a] Feng Li [a]*

[a] State Key Laboratory of Chemical Resource Engineering, Beijing University of Chemical Technology, Box 98, Beijing 100029, China

[b] Quzhou Institute for Innovation in Resource Chemical Engineering, Quzhou, 324000, China

* To whom all correspondence should be addressed

E-mail: fangl@mail.buct.edu.cn (G. Fan); lifeng@mail.buct.edu.cn (F. Li)

Experimental section

Synthsis of samples

Synthesis of Fe_2O_3-TiO_2 sample with a 4 wt % Fe loading. Initially, 2.02 g of Fe $(NO_3)_3 \cdot 9H_2O$ was dissolved in 40 mL of deionized water under magnetic stirring until a clear solution was obtained. Subsequently, 40 mL of 0.5 M NaOH solution was added and the resulting solution was stirred continuously for 30 min. Then, the resulting suspension was transferred to a 100 mL Teflon-lined autoclave and subjected to hydrothermal treatment at 150 °C for 12 h. The precipitate was collected by centrifugation, washed three times with deionized water, dried overnight at 60 °C, and calcined at 400 °C for 4 h to obtain Fe_2O_3. Then, 2 mmol of the synthesized Fe_2O_3 and 0.4 g of TiO_2 were ultrasonically dispersed in 50 mL of deionized water for 1 h to form a suspension. This suspension was then transferred to a three-necked flask and stirred continuously while the solvent was evaporated in an oil bath at 60 °C. The resulting solid was calcined at 500 °C for 4 h, yielding the final product (designated as 4% Fe_2O_3-TiO_2).

Determidation of the light intensity in the PCR reaction.

The light intensity in the PCR reaction was determined with a calibrated optical power meter (CEL-NP2000, Beijing China Education Au-light Co., Ltd.). After turning on the light source and waiting until the light spot stabilized, the light intensity was measured at the center of the xenon lamp spot and at four peripheral positions. The average value was then calculated, yielding a light intensity of 183.3 $mW \cdot cm^{-2}$ under our experimental conditions. Although the light intensity was not adjusted to 1 Sun (100 $mW \cdot cm^{-2}$), the height of the Xe lamp was kept constant for all reactions, ensuring that the light intensity remained identical for each experiment.

Calculation details

The adsorption energy of a CO_2 or a CO molecule (E_{ads}) and Gibbs free energies for each gaseous and adsorbed species could be calculated by the following equations 1 or 2:

$$E_{ads} = E(CO_2/slab) - E(slab) - E(CO_2\ (gas)) \quad (1)$$

$$E_{ads} = E(CO/slab) - E(slab) - E(CO\ (gas)) \quad (2)$$

Where $E(CO_2/slab)$ or E(CO/slab) represented the total energy for a CO_2 or CO molecule

adsorbed on the catalyst, E(slab) was the energy of the bare slab, and E (CO_2 (gas)) or E (CO (gas)) was the energy of gas phase CO_2.

Gibbs free energies for each gaseous and adsorbed species were calculated at 298.15 K, according to the equation 3:

$$G = E_{DFT} + E_{ZPE} - TS \quad (3)$$

where E_{DFT} was the electronic energy of reactants or products calculated from DFT, E_{ZPE} was the zero-point energy obtained from frequency analysis, S was the entropy change, and T was the thermodynamic temperature (298.15 K)

Figure and Tables

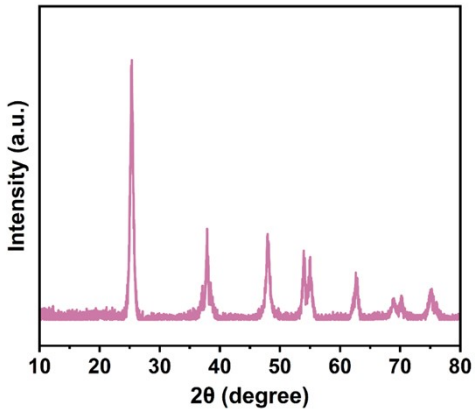

Fig.S1 XRD spectra of the samples after heat treatment at 500℃

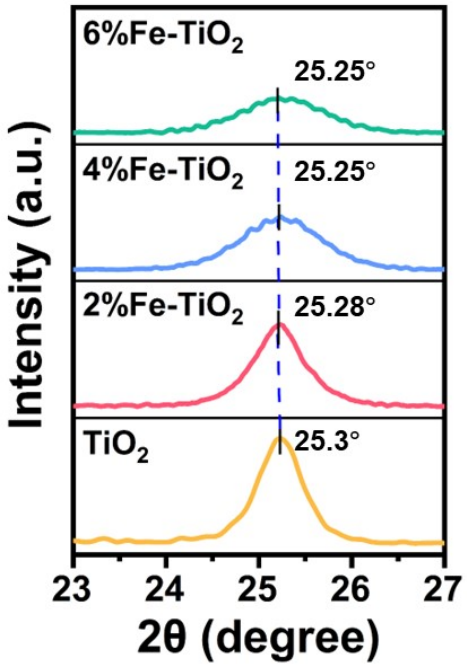

Fig.S2 Change in peak position of anatase TiO2 (101) crystal plane for TiO_2, 2% Fe-TiO_2, 4% Fe-TiO_2 and 6% Fe-TiO_2 samples.

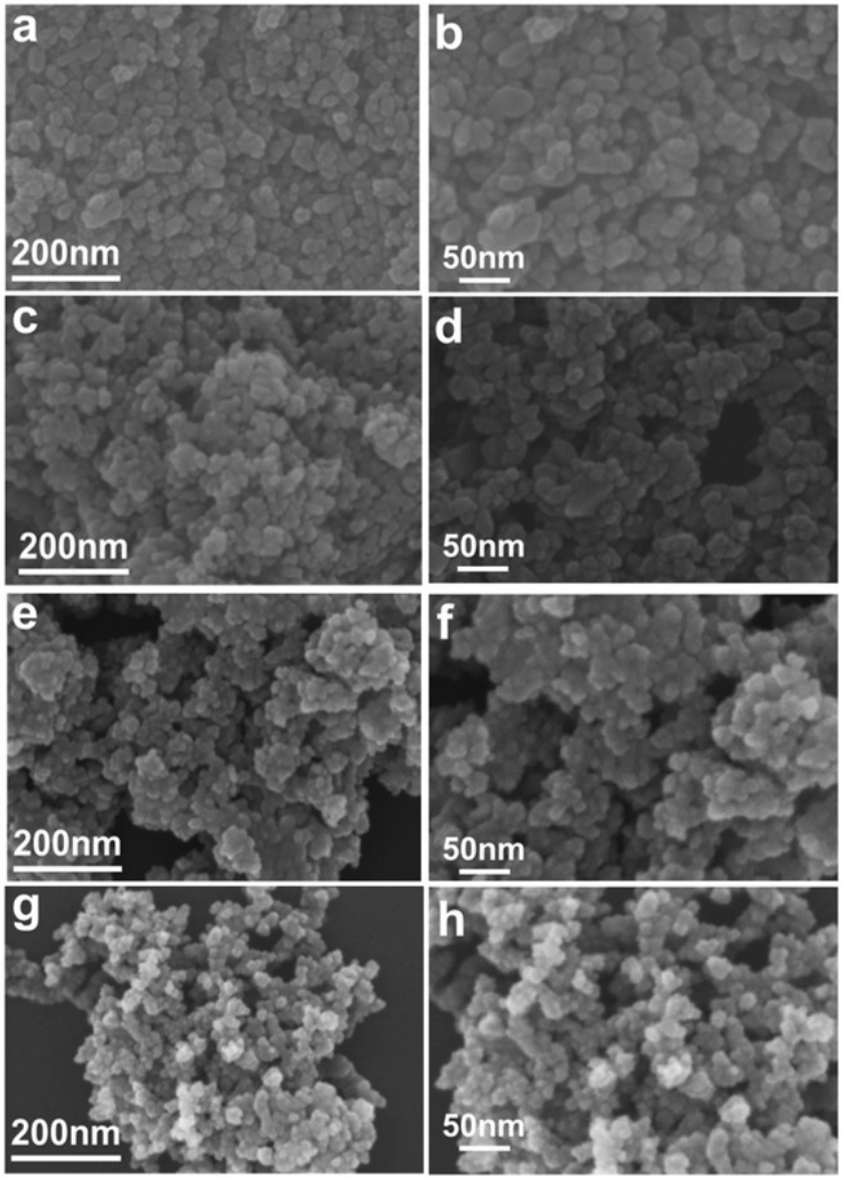

Fig.S3 SEM images of TiO_2(a, b), 2% Fe-TiO_2 (c, d), 4% Fe-TiO_2 (e, f), and 6% Fe-TiO_2 (g, h) samples.

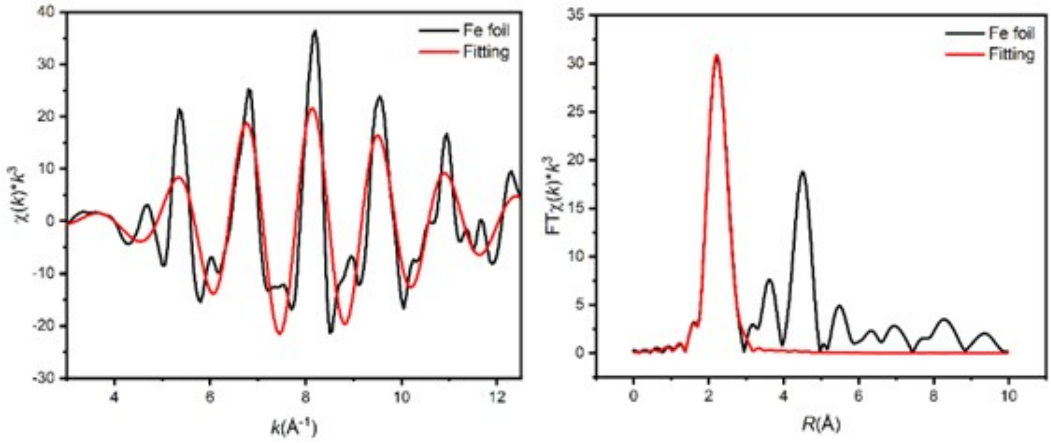

Fig.S4 Fe K-edge EXAFS oscillations of Fe foil (left) and FT-EXAFS fitting results of Fe foil (right).

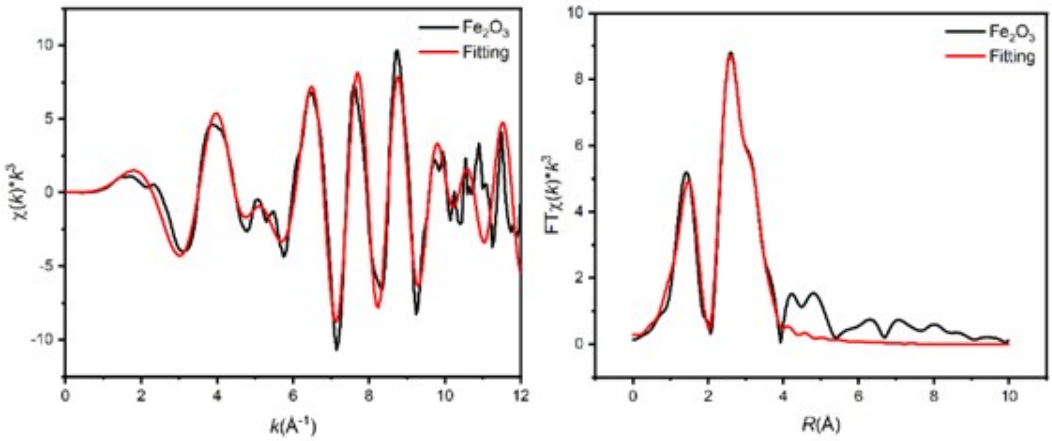

Fig.S5 Fe K-edge EXAFS oscillations of Fe_2O_3 (left) and FT-EXAFS fitting results of Fe_2O_3 (right).

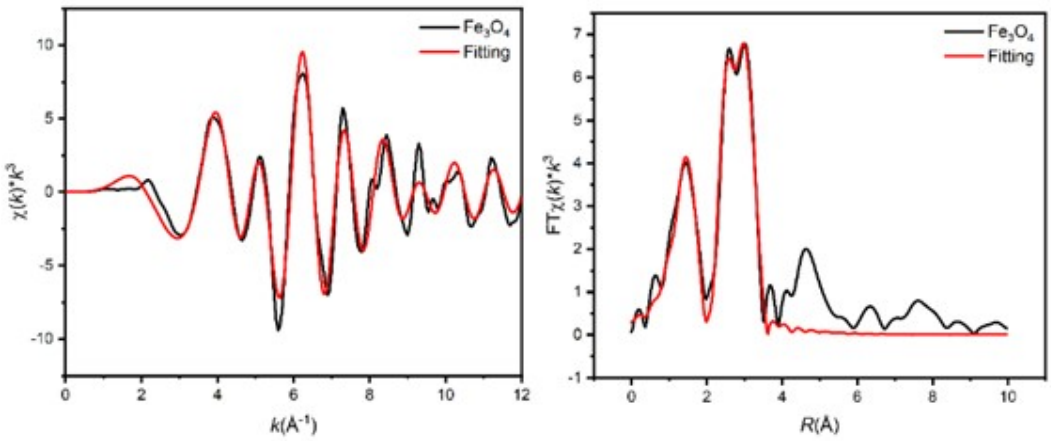

Fig.S6 Fe K-edge EXAFS oscillations of Fe_3O_4 (left) and FT-EXAFS fitting results of Fe_3O_4 (right).

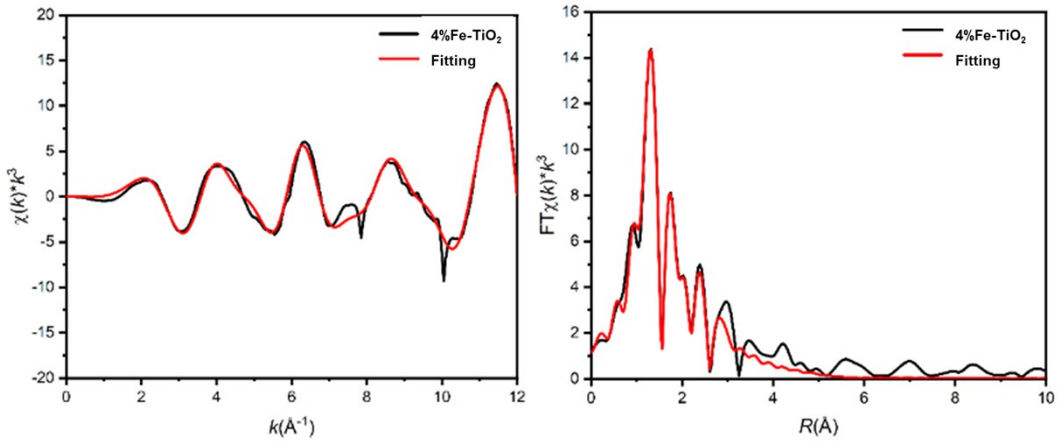

Fig.S7 Fe K-edge EXAFS oscillations of 4%Fe-TiO_2 (left) and FT-EXAFS fitting results of 4%Fe-TiO_2 (right).

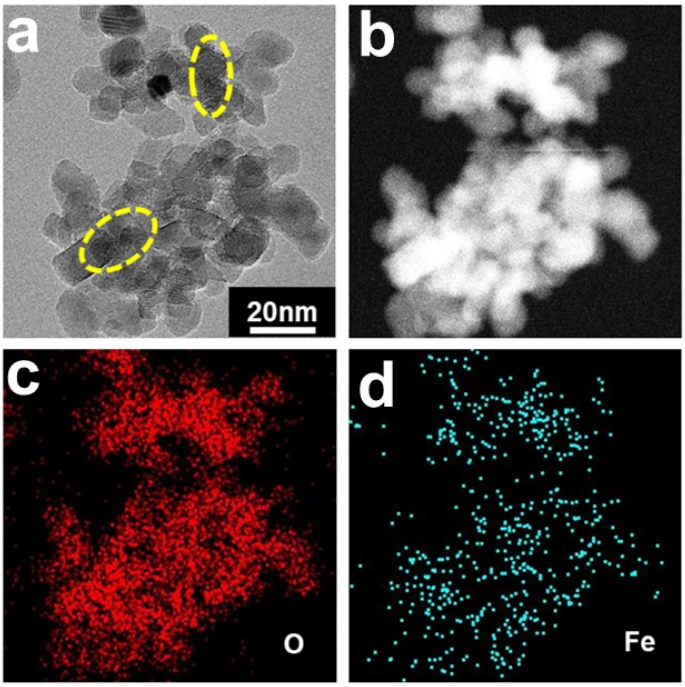

Fig.S8 TEM image, HAADF-STEM image, and corresponding elemental mapping of O and Fe elements of the 6% Fe-TiO_2 sample. In yellow oval-shaped areas in (a), some surface aggregated Fe-containing species can be observed.

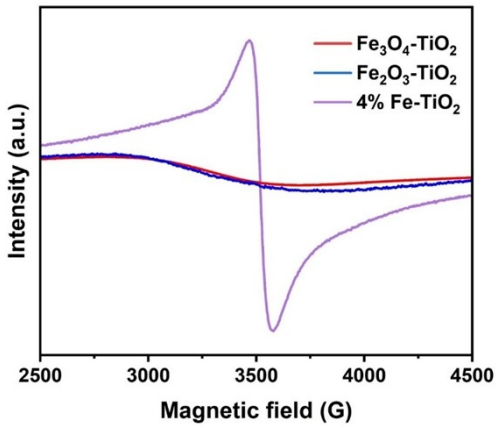

Fig.S9 EPR spectra of Fe_3O_4-TiO_2, Fe_2O_3-TiO_2, and 4% Fe-TiO_2 samples.

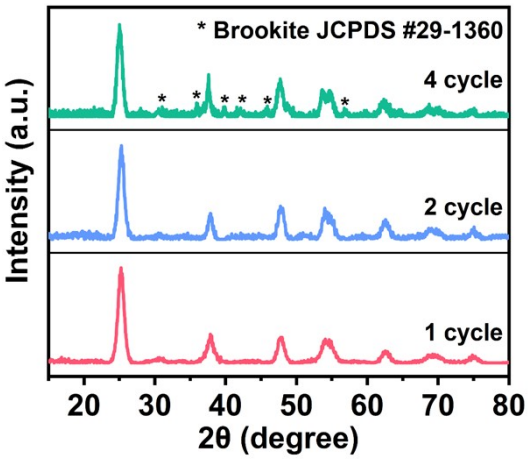

Fig.S10 XRD patterns of 4% Fe-TiO_2 catalyst before and after1, 2, 4 cycle.

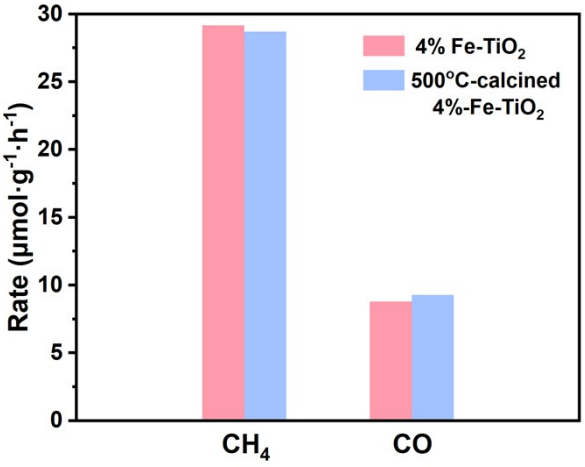

Fig.S11 comparison of CH_4 and CO evolution rates in the PCR reaction over 4%Fe-TiO_2 and 500°C-calcined 4%Fe-TiO_2 catalysts.

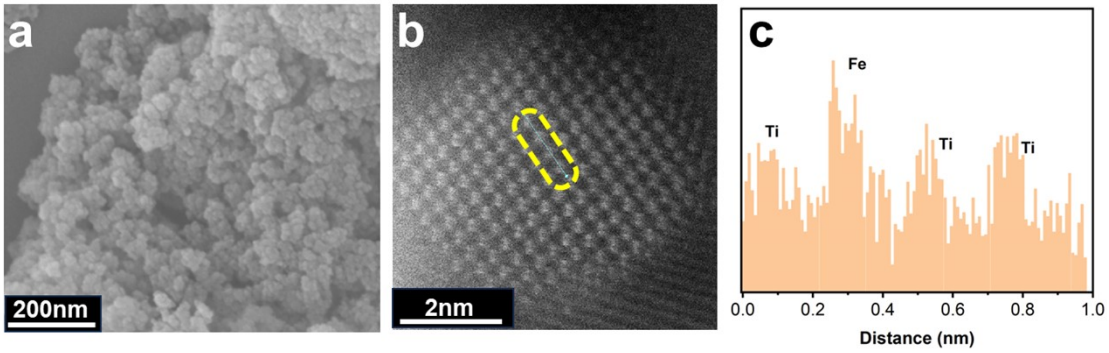

Fig.S12 SEM image of 4%Fe-TiO_2 after four reaction cycles (a). HAADF-STEM image of Fe-TiO_2 after reaction (b) and corresponding intensity profiles along the yellow line (c).

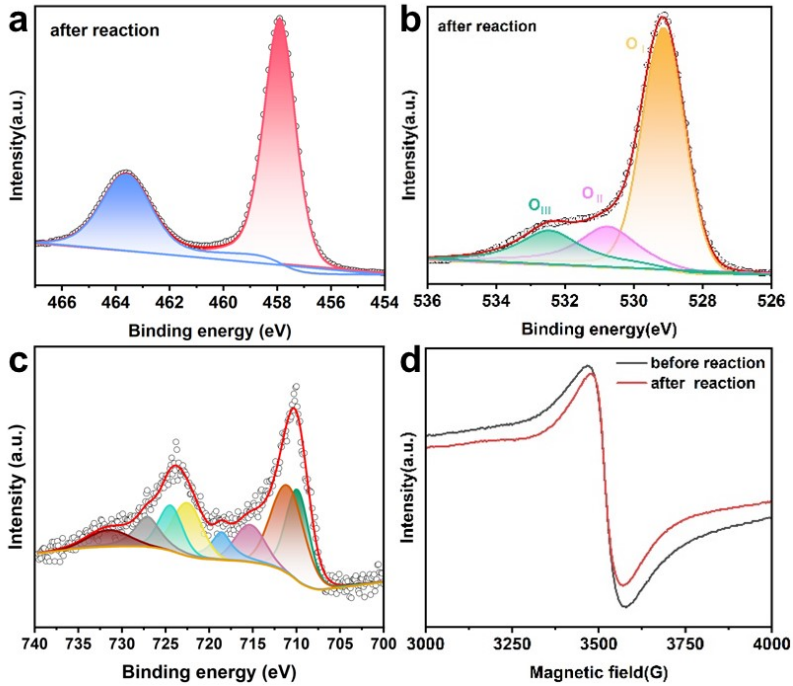

Fig.S13 XPS spectra of Ti 2p (a), O1s (b), Fe 2p (c) and EPR pattern (d) of the 4% Fe-TiO_2 sample after four reaction cycles.

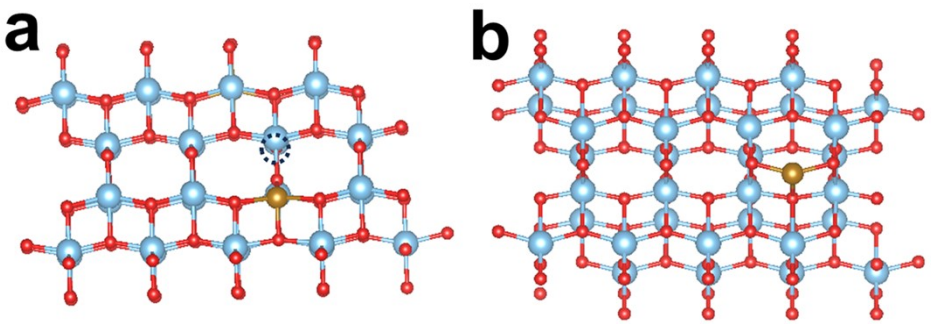

Fig.S14 The models of Fe-TiO_2 with single Fe atom doped into the TiO_2 lattice support surfaces (a) and single Fe atom supported on the terrace of TiO_2 surface (b) (brown, blue, red, and black dashed circle denote Fe, Ti, O, and Ov, respectively).

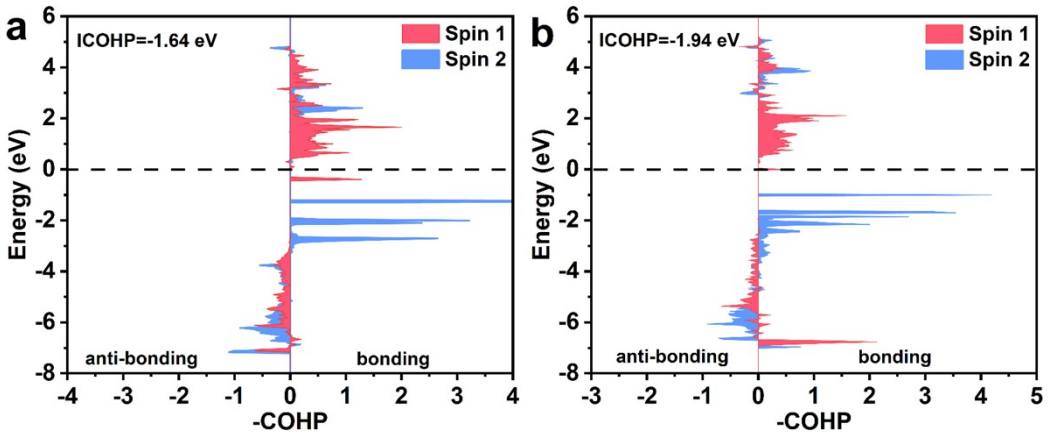

Fig.S15 Fe-O bond binding energy versus COHP values of Fe-O interactions in Fe-supported (a) and Fe-doped (b) models.

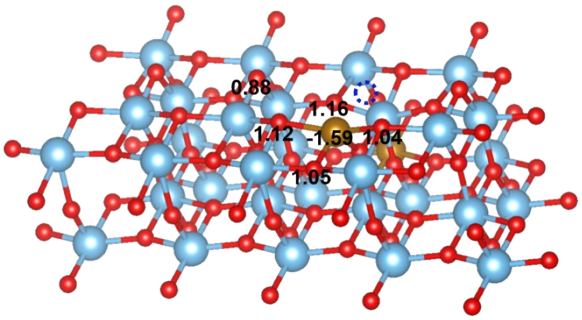

Fig.S16 Bader charge analysis of 4%Fe-TiO_2 (The blue circle indicates oxygen vacancy).

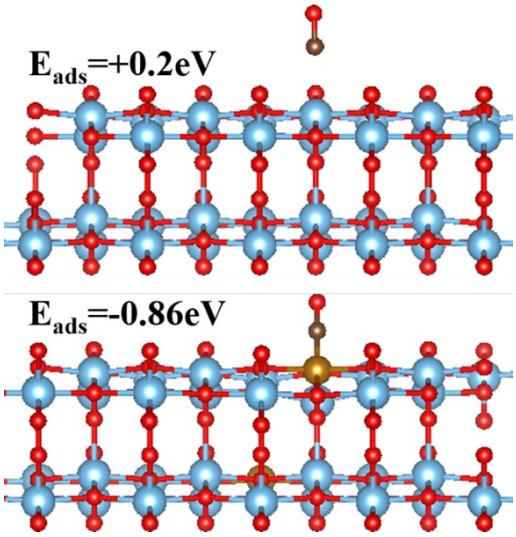

Fig.S17 TiO_2 adsorption of CO model (top) and 4% Fe-TiO_2 adsorption of CO model (bottom).

Table S1 Elemental analysis results of different Fe-TiO_2 samples.

Samples	Fe content [a] (wt%)	Fe content [b] (wt%)
2%Fe-TiO_2	2.0	1.988
4%Fe-TiO_2	4.0	3.8374
6%Fe-TiO_2	6.0	5.9887

[a] Theoretical iron content. [b] Actual iron content determined by the ICP-OES analysis.

Table S2 EXAFS fitting parameters at the Fe K-edge for different catalysts.

Samples	Shell	CN [a]	R(Å)[b]	σ^2 [c]	ΔE_0 [d]	R factor [e]
Fe foil	Fe-Fe	8	2.478±0.004	0.00534	7.785±0.9	0.00091
	Fe-Fe	6	2.854±0.011	0.00747		
	Fe-O	6.7±0.4	1.988±0.01	0.01594		
Fe_2O_3	Fe-Fe	3.3±0.3	2.934±0.011	0.00496	-4.958±0.5	0.00957
	Fe-Fe1	2.1±0.4	3.378±0.005	0.00541		
	Fe-Fe2	2±0.3	3.678±0.021	0.00104		
	Fe-O	5.8±0.2	1.986±0.01	0.01573		
Fe_3O_4	Fe-Fe	3.8±0.3	2.977±0.01	0.01114	-7.351±0.2	0.00437
	Fe-Fe	9±0.4	3.475±0.004	0.01067		
	Fe-O	5.4±1.1	1.997±0.012	0.01274		
Fe-TiO_2	Fe-Ti	0.8±0.4	2.522±0.08	0.01882	-0.86±0.95	0.0138
	Fe-Ti	1.9±0.6	3.065±0.05	0.00944		

a CN: coordination numbers; b R: bond distance; c σ^2: Debye-Waller factors; d ΔE_0: the inner potential correction. e R factor: goodness of fit.

Table S3 Kinetic analysis of emission decay time

samples	τ_1	τ_2	τ_{ave}（ns）	A_1	A_2
TiO_2	0.5091	3.6304	1.8638	972.0574	104.4302
4%Fe-TiO_2	0.8325	5.4817	3.3351	899.6824	159.2908

$$\tau_{ave} = \frac{A_1\tau_1^2 + A_2\tau_2^2}{A_1\tau_1 + A_2\tau_2}$$

Table S4 Band structures of different photocatalysts

Samples	Eg (eV)	CB (eV)	VB (eV)
TiO_2	3.28	-0.63	2.65
2%Fe-TiO_2	3.06	-0.56	2.5
4%Fe-TiO_2	2.87	-0.57	2.3
6%Fe-TiO_2	2.75	-0.53	2.22

Table S5 Catalytic performance of photocatalysts for CO_2 reduction to CH_4

Catalysts	Light source	Light intensity ($mW \cdot cm^{-2}$)	Reaction medium	$Sel._{CH4}$ (%)	CH_4 production rate ($\mu mol\ g^{-1}\ h^{-1}$)	Refs.
PdCu alloy on 2D TiO_2 nanosheets	300W Xe lamp (AM 1.5G filter)	~100	Gas-solid H_2O	98.7	18.1	[1]
Fe-porphyrin/TiO_2-x	300 W Xe lamp (＞420 nm)	-	Gas-solid H_2O	56.1	20.48	[2]
CuO-TiO_2	125 W mercury UVA lamp (＞366 nm)	5	Gas-solid H_2O	98	23.0	[3]
Ag/TiO_2	8 W Hg lamp (254nm)	-	Gas-solid H_2O	48	8.5	[4]
Pd/TiO_2	500 W Hg lamp (＞310 nm)	-	Gas-solid H_2O	67	1.415	[5]
CdS/TiO_2	300 W Xe lamp (full spectrum)	-	Gas-solid H_2O	100	11.9	[6]
$ZnIn_2S_4$/TiO_2 nanobelts	300 W Xe lamp (AM 1.5G filter)	~100	Gas-solid H_2O	100	1.135	[7]
Au@TiO_2-20-Au	200W Hg/Xe lamp (UV+Vis)	-	Gas-solid H_2O	100	6	[8]
Au/TiO_2	125 W mercury UVA lamp (＞366 nm)	5	Gas-solid H_2O	60	15	[3]
TiO_2@PDA	350W Xenon lamp (AM 1.5G filter)	~100	Gas-solid H_2O	90	1.5	[9]
Pd/TiO_2	150 W Xe lamp (＞400nm)	65.0 and 40.5	Gas-solid H_2O	68	3.7	[10]
500-TiO_{2-x}	300 W Xe lamp (AM 1.5G filter)	~100	Gas-solid H_2O	74	14.3	[11]
H-TiO_{2-x}	300 W Xe lamp (AM 1.5G filter) and (400-780nm)	~100	Gas-solid H_2O	79	16.2	[12]
Ru-TiO_{2-x}	300 W Xe lamp (AM 1.5G filter)	~100	Gas-solid H_2O	91	31.63	[13]
MoS_2/TiO_2	350W Xe arc lamp (AM 1.5G filter)	~100	Gas-solid H_2O	53	2.86	[14]
Ti^{3+}/TiO_2	300W Xe arc lamp (＞420nm)	216	Gas-solid H_2O	34	11.9	[15]

Cu/TiO_2 (001)	300 W Xe lamp	-	Gas-solid H_2O	94	40.3	[16]
Pd-HPP-TiO_2	300 W Xe lamp (325-780nm)	-	Gas-solid H_2O	59	48	[17]
4%Fe-TiO_2	300 W Xe lamp (320-780nm)	183.3	Gas-solid H_2O	93	29.2	**This work**

References

1. Y. Liu, S. Sun, M. Ma, X. Zhong, F. Gao, G. Hai and X. Huang, *J. Mater. Chem. A*, 2024, **12**, 23577-23589.
2. Y. Wu, L. Yan, Y. Yu and C. Jing, *Catal. Sci. & Technol.*, 2021, **11**, 6103-6111.
3. A. Olivo, E. Ghedini, P. Pascalicchio, M. Manzoli, G. Cruciani and M. Signoretto, *Catalysts*, 2018, **8**, 41.
4. K. Kočí, K. Matějů, L. Obalová, S. Krejčíková, Z. Lacný, D. Plachá, L. Čapek, A. Hospodková and O. Šolcová, *Appl. Catal. B*, 2010, **96**, 239-244.
5. R. Camarillo, S. Tostón, F. Martínez, C. Jiménez and J. Rincón, *J. Supercrit. Fluids*, 2017, **123**, 18-27.
6. J. Low, B. Dai, T. Tong, C. Jiang and J. Yu, *Adv. Mater.*, 2019, **31**, 1802981.
7. G. Yang, D. Chen, H. Ding, J. Feng, J. Z. Zhang, Y. Zhu, S. Hamid and D. W. Bahnemann, *Appl. Catal. B*, 2017, **219**, 611-618.
8. A. Pougin, G. Dodekatos, M. Dilla, H. Tüysüz and J. Strunk, *Chem. Eur. J.*, 2018, **24**, 12416-12425.
9. A. Meng, B. Cheng, H. Tan, J. Fan, C. Su and J. Yu, *Appl. Catal. B*, 2021, **289**, 120039.
10. A. Nishimura, T. Inoue, Y. Sakakibara, M. Hirota, A. Koshio and E. Hu, *Molecules*, 2020, **25**, 1468.
11. G. Yin, Q. Bi, W. Zhao, J. Xu, T. Lin and F. Huang, *ChemCatChem*, 2017, **9**, 4389-4396.
12. G. Yin, X. Huang, T. Chen, W. Zhao, Q. Bi, J. Xu, Y. Han and F. Huang, *ACS Catal.*, 2018, **8**, 1009-1017.
13. Y. Zhou, Q. Zhang, X. Shi, Q. Song, C. Zhou and D. Jiang, *J. Colloid Interface Sci.,* 2022, **608**, 2809-2819.
14. F. Xu, B. Zhu, B. Cheng, J. Yu and J. Xu, *Adv. Opt. Mater.*, 2018, **6**, 1800911.
15. X. Xin, T. Xu, L. Wang and C. Wang, *Sci. Rep.*, 2016, **6**, 23684.
16. D. Li, Q. Li, Y. Zhou, Q. Zhang, Q. Ye, R. Yang and D. Jiang, *Inorg. Chem.*, 2024, **63**, 15398-15408.
17. Y. Ma, X. Yi, S. Wang, T. Li, B. Tan, C. Chen, T. Majima, E. R. Waclawik, H. Zhu and J. Wang, *Nat. Commun.*, 2022, **13**, 1400.